Nickel-Iron-Aluminium Shape Memory Alloys with Improved Properties by Rapid Solidification

P. Johansson, J. Liu and S. Savage
Swedish Institute for Metals Research
Drottning Kristinas väg 48
S-114 28 Stockholm, Sweden

Rapidly solidified micro-wires (~ 150 μm dia) and ribbons (~ 75 μm thick) have been produced by direct casting and melt spinning techniques respectively. The alloys studied have the composition $(Ni_xFe_yAl_z)_{99.8}B_{0.2}$, where x = 0.57-0.62; y=0.09-0.14; z=0.245-0.29. The alloys have been characterized by thermal analysis (DSC), electrical resistance measurement, tensile testing and microstructural analysis.

A range of alloy compositions have been produced. All of them exhibit the shape memory effect (shape recovery on heating, after cold deformation) although by DSC the martensite transformation is not clearly seen in all the alloys. Measurement of electrical resistance is the most sensitive way to follow the transformations in these alloys. The difference in resistance, at the same temperature, can be as high as 0.245 μΩm for heating and cooling cycles. The maximum fracture stress obtained in an as-cast wire is ~ 1450 MPa, with elongation to fracture in the range 14-18%.

Estimated values of pseudo-elasticity are as high as 14%. Microstructural analysis leads to the conclusion that the ribbons experience a higher solidification rate than the wires, which may explain the somewhat different martensite properties.

Introduction

Shape memory alloys (SMA's) have many potential applications in functional areas for control systems, robotics, electronics, telecommunications and biomedicine. However, to produce the alloys in a suitable form (wire or thin strip) by conventional metal working processes is often difficult due to the poor workability of these alloys. Rapid solidification technology (RST) offers a convenient and economical alternative way to produce near net shape materials. The rapidly solidified shape memory alloys usually have a high area/-volume ratio which enhances heat transfer to and from the materials. It has been shown (1) that metastable nickel-rich β martensite (β') obtained by water quenching from the β-phase field at high temperature undergoes a thermoelastic martensite transformation (β'→β) at elevated temperatures, leading to a shape memory effect. However, conventionally cast NiAl compound does not exhibit an appreciable tensile elongation at room temperature and hence the shape recovery has been limited to a small bending strain field (2). Ni_3Al (γ') and γ'+β compounds in the Ni-Fe-Al system with good ductility and high strength have been obtained by rapid solifification (3,4). Furukawa et al (5) have investigated of the Ni-Fe-Al system which shows a great potential for development of SMA's due to extension of the β- and β'-phase field by RST.

It was reported (5), that the transformation between β' and β occurs reversibly in a rather narrow temperature range of about 80K. Addition of 0.17 at% B to $Ni_{33}Fe_{14}Al_{23}$ increases the fracture strenght from 394 to 1100 MPa and elongation from 2.8% to 18.1%, while the yield strength remains unchanged.

The reason for the improvement of ductility and strength is probably a combined effect of grain size refinement and suppression of the development of an ordered structure combined with grain boundary segregation. Significant deterioration of the shape memory effect (SME) and ductility in the vicinity of 600 K was found to be due to the precipitation of Ni_3Al and Ni_2Al_3.

The present work aims at further development of these newly found Ni-Fe-Al-base shape memory alloys by RST. The products were characterized by microstructure analysis, tensile testing and transformation temperature measurement by differential thermal calorimetry (DSC) and electrical resistance measurement.

Experimental work

The compositions of the rapidly solidified ribbons and wires are shown in Table 1 produced by "chill block melt spinning" and "in rotating water melt spinning" (6) respectively.

Alloy	Ni	Fe	Al	B
1	56.90	13.98	28.95	0.17
2	61.66	13.70	24.47	0.17
3	61.89	8.98	28.95	0.17
4	59	14	27	
5	58.90	13.98	26.95	0.17

Table 1. Investigated alloys. Content at%.

Nickel, aluminium, iron and boron were weighed out for each alloy and induction melted under an argon atomsphere in an alumina crucible. The molten metal was sucked up in a silica tube and allowed to solidify. After cooling in water, and removing the silica tube 5 mm diameter rods were obtained. These were cleaned in alcohol, and dried in hot air and cut up into small pieces for the wire casting and melt spinning experiments. Wires of ~ 150 μm dia., and ribbons of ~ 75 μm thickness were produced (6).

Samples for optical microscopy were prepared by conventional mounting in thermosetting resin, grinding, polishing and chemical etching. Tensile testing was carried out at a strain rate of $4.17 \cdot 10^{-4}$ s^{-1} at room temperature. Differential thermal calorimetry (DSC) was performed on ~15 mg samples at a cooling/heating rate of 10 K/s. Electric resistivity measurements were performed on as-cast and as cast and heat treated samples.

Results and discussion

DSC

All the alloys show a visible shape recovery on heating after cold deformation. However, only two of the ribbons (alloys 4 and 5) show peaks on the DSC-curves, indicating a phase transformation. The difference between these two ribbons is only 0.17 at % boron addition. The measured transformation temperatures correlate well with the microstructure shown in Figure 1. With the predicted transformation temperatures in mind (5) alloy no. 3 ought to show martensite phase but didn't. No DSC-peak was observed, neither below or above

room temperature, in spite of the fact that tests with different thickness of the ribbon were done. The conclusion of this is that without carefully noted conditions during rapid solidification, it is hard to predict the shape of the metastable phase-diagram. Also alloy no. 2 was predicted to show DSC peaks but didn't.

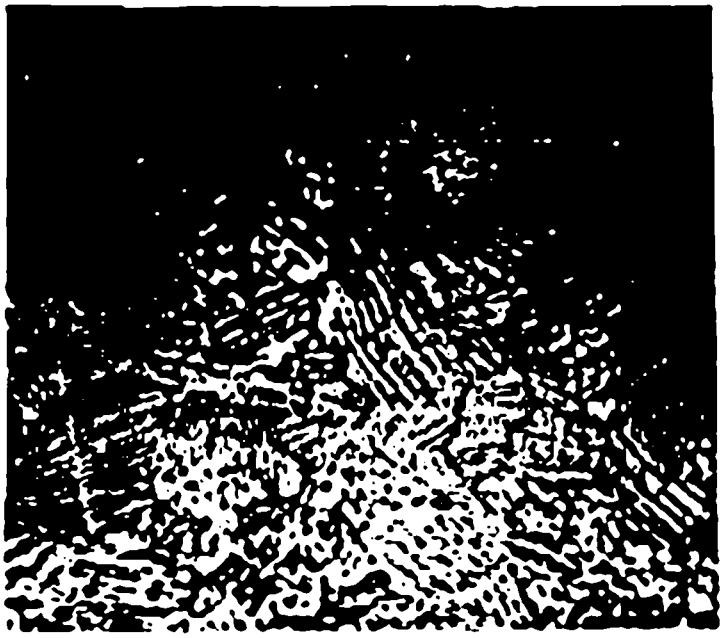

Figure 1. Ribbon of alloy No. 5.

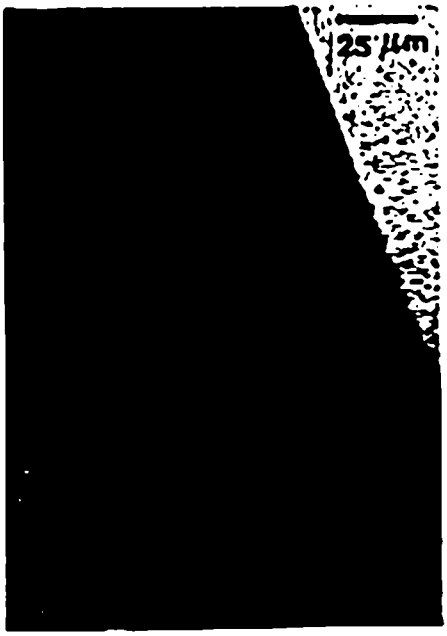

Figure 2. Wire of alloy No. 5.

the rapidly solidified wires show a completely different behaviour. They show no peaks at all in the DSC. A typical microstructure is shown in Figure 2. Alloys with no DSC peaks in ribbon form are not expected to show peaks for the wire. For the two alloys for which peaks were obtained in the ribbon very slight peaks can be seen by careful examination. The conclusion which may be drawn is that a high cooling rate is the dominant factor for obtaining martensite in these alloys.

Heat treatment

After annealing ribbons of alloy no. 5 for 1 hour a DSC-run was carried out which gave the results shown in Figure 3 and 4. The martensite to austenite peak transition temperature A* is lowered from 425K in the as quenched state to 380K after the heat treatment at 623K, but then raised to 405K after annealing at 803K.

It is surprising that A* versus the heat treatment temperature T_a at 800K diverge from previously reported results (5). The ΔH dependence on T_a shows that the volume of transformation is reduced after heat treatment, and decreases with increasing annealing temperature due to stabilization of equilibrium phases. Thermal cycling between 300K and 500K was carried out with wire of alloy no. 4 to find out if this can force a peak to appear, without result.

Metallography

The results from optical microscopy are given in Tables 2 and 3. In Figure 1 the presence of martensite in the ribbon of alloy no. 5 is clearly seen. The same phase is observed in ribbons of alloy no. 4.

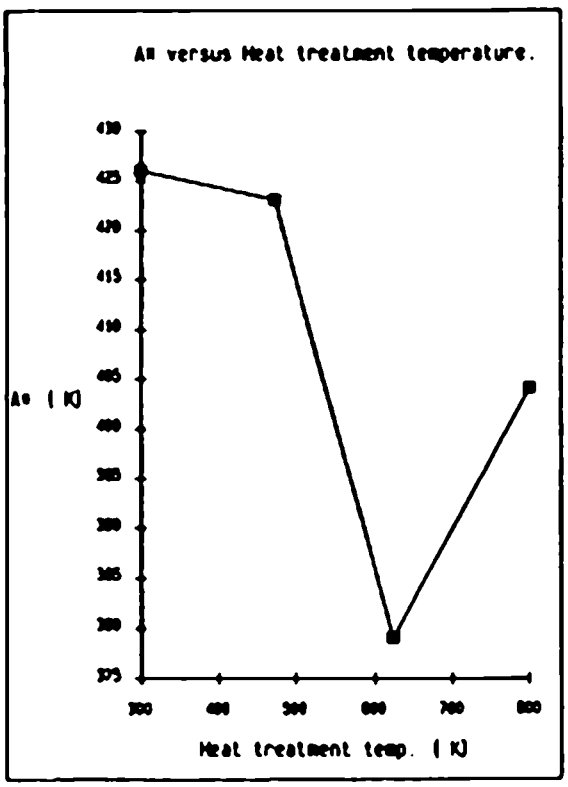

Figure 3. Ribbon of alloy No. 5. Heat treated for 1 hour.

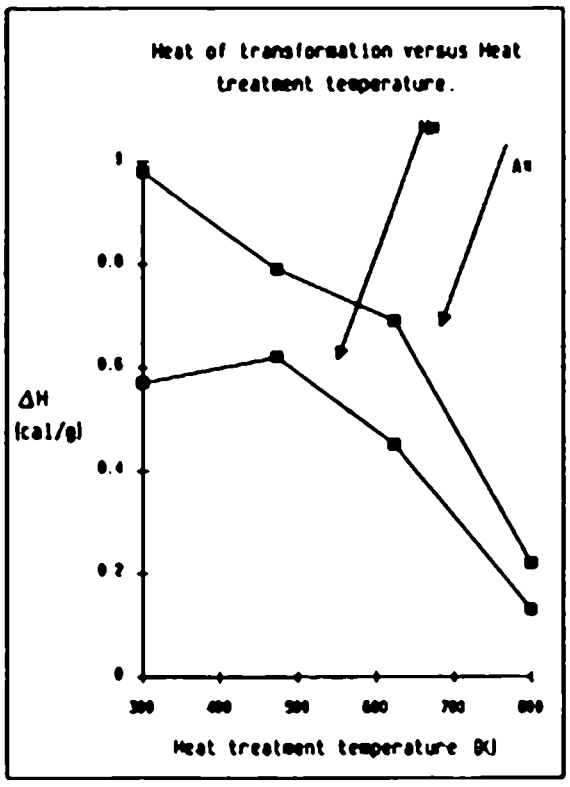

Figure 4. Ribbon of alloy No. 5. Heat treated for 1 hour. M* and A* are austenite to martensite and marteniste to austenite peak transition temperatures respectively.

Alloy	Roller velocity (m/s)	Mean thickness (μm)	Mean width (μm)	Cell size (μm)	Mechanical property Max R_m (N/mm²)	Max $R_{p0.2}$ (N/mm²)	Max ϵ_f (%)
1	10	123	1099	12.7*	-	-	-
2	6	110	960	-	980	530	10.5
3	6	152	1428	16.2*	-	-	-
4	15	41	1450	7.1	204	165	1.9
5	15	50	695	8.3	211	161	1.5

* at roller side.

Table 2. Experimental conditions and properties of rapidly solidified directly cast ribbons.

In Figure 5 a schematic relationship between the austenite to martensite transition start temperature M_s and Al-content is shown. The microsegregation in the wires results in a microstructure that consists of primary solidified dendrites and secondary solidified phase with increased Al-content, as can be seen in Figure 2. This gives rise to a range of transformation temperatures, and as a result a poor SME is obtained.

Alloy	Mean wire diameter (μm)	Mean secondary dendrite arm spacing (μm)	Mechanical property Max R_m (N/mm^2)	Max $R_{p0.2}$ (N/mm^2)	Max ϵ_f (%)
1	175	3.4	-	-	-
2	179	1.8	1015	279	13.3
3	243	3.0	-	-	-
4	118	2.3	526	422	4.4
5	183	2.4	1448	519	18

Table 3. Properties of rapidly solidified directly cast micro-wires.

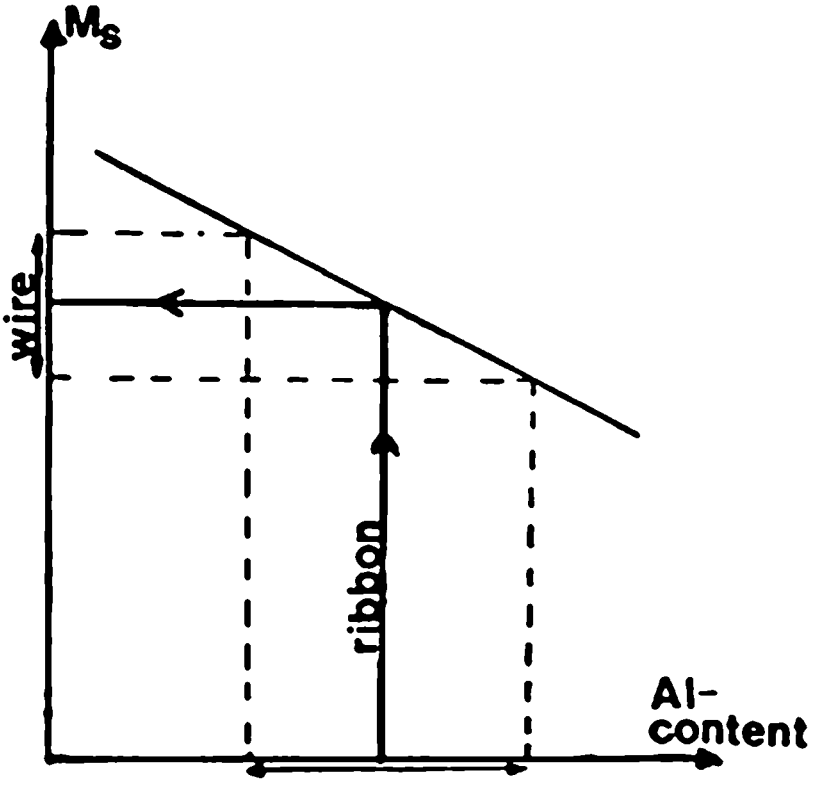

Figure 5. The micro-segregation effect on M_s.

By measurement of the secondary dendrite arm spacing or cell size it is possible to calculate cooling rates of the as-quenched ribbons. The cooling rate in this process is normally in the range of 10^5-10^6 K/s (7). The secondary dendrite arm spacings in the wires give a cooling rate of ~10^4 K/s (8) which is somewhat lower than for ribbons. To obtain cooling rates in wire comparable with ribbon, which are needed in order to obtain the same microstructure, the heat transfer has to be improved, for example, by casting wire of smaller diameter.

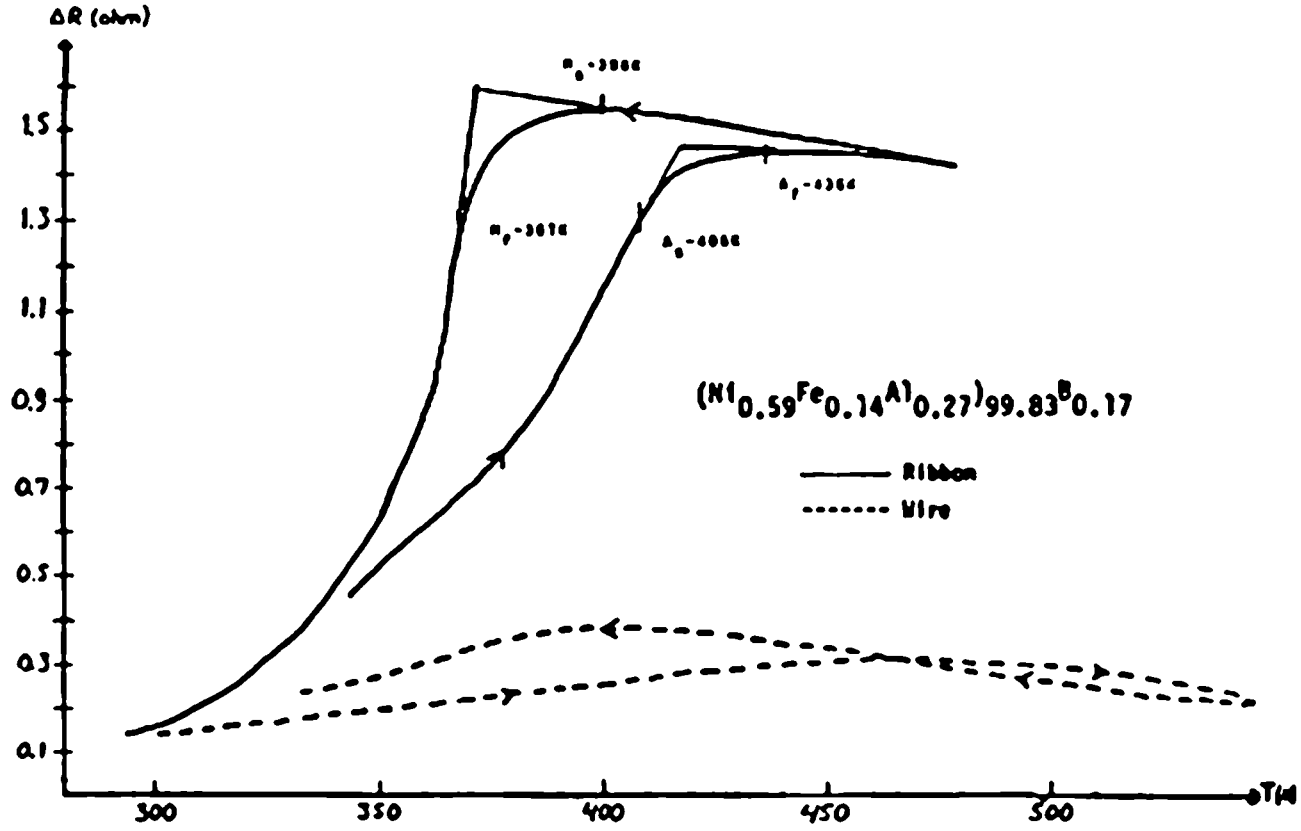

Figure 6. Resistance measurements. Interpretation of transformation.

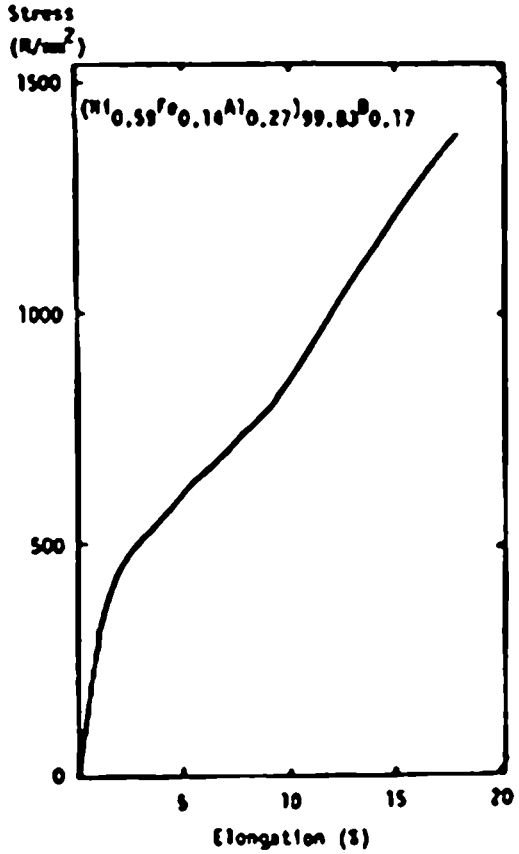

Figure 7. Stress - Strain diagram.

Resistance measurements

Resistance versus temperature results for ribbon and wire are given in Fig.6. For alloy no. 4, it is possible to find M_s=400K and M_f=382K (consistent with DSC results which gives M_s=399K and M_f=379K). On heating it is much more difficult to observe accurately but gives values of A_s=429K and A_f=451K (DSC results gives A_s=410K and A_f=436K). The agreement between these results is encouraging. For ribbon of alloy no.5 it is even more encouraging with M_s=396K M_f=367K, A_s=406K and A_f=436K. (DSC gives 397, 374, 404 and 441K respectively). To interpretate the curves help is taken from the DSC-results. In Figure 6 it is shown how M_s, M_f, A_s and A_f have been obtained from the heating and cooling curves. In this figure wire and ribbon are compared. The difference in resistance, at the same temperature, can be as high as 0.245 μΩm for heating and cooling cycles.

Tensile testing

The tensile testing results are shown in Tables 2 and 3 for alloys no 2, 4 and 5. These results make it clear that the wires and ribbons found ductile by a simple bend test (bending the ribbon or wire 180°, to give a strain of 1) also give high tensile strengths e.g. for wires and ribbons of alloy no. 2 and wires of alloy no. 5. A large scatter of tensile results was observed which is a result of variations in thickness of samples and the production conditions (for example roughness of the ribbon surface). All ribbons and wires were tested in the as-produced condition.

The highest mechanical testing results are those shown in Figure 7, obtained from wire of alloy no. 5. A fracture elongation as high as 18 % combined with 1448 MPa ultimate tensile strength are comparable to results in (5). A value for recoverable strain (6), is estimated at about 14%.

Conclusions

The mechanical and shape memory properties show significant variations in terms of small differences in alloy content, cooling rate and microstructure. The compositional dependence of rapidly solidified structures in the Ni-Fe-Al system can not be estimated without careful evaluation of the production process parameters, e.g. cooling rate.

Microsegregation in the wires results in a microstructure that consists of primary solidified dendrites and secondary solidified phase with increased Al-content. As a result of this a poor SME is obtained. With further development of the processing techniques for these alloys, on the basis of the results shown, it is expected that wires and ribbons with good combinations of mechanical properties and SME can be produced.

Acknowledgement

This work has been sponsored by National Swedish Board for Technical Development (STU). Fruitful suggestions and discussions with Prof. A. Inoue of the Institute for Materials Research, Tohoku University and Prof. H. Fredriksson of the Royal Institute of Technology, Stockholm, are gratefully acknowledged.

References

(1) K. Enami and A. Nenno, Metall. Trans. 2 (1971) 1487.

(2) Y.K. Au and C. M. Wayman, Scr. Metall., 6 (1972) 1209.

(3) A. Inoue, H. Tomioka and T. Masumoto, Metall. Trans. 14 (1983) 1367.

(4) A. Inoue, H. Tomioka, T. Masumoto, J. Mater. Sci. 19 (1984) 3097.

(5) S. Furukawa, A. Inoue and T. Masumoto, Mater. Sci. Eng., 98:2(1988), 515-518.

(6) P. Johansson, report No. IM-2398, (Dec. 1988). Internal report from the Swedish Institute for Metals Research, Stockholm.

(7) R. Ruhl, Materials Science Engineering 1 (1967) 313-320.

(8) I. Ohnaka, International Journal of Rapid Solidification, 1 (1984-85) 219-236.